Fault strength in thin-skinned tectonic wedges across the smectite-illite transition: Constraints from friction experiments and critical tapers

Telemaco Tesei[1], Brice Lacroix[2], and Cristiano Collettini[1,3]
[1]Istituto Nazionale di Geofisica e Vulcanologia, Via di Vigna Murata 605, 00143 Rome, Italy
[2]Department of Earth and Environmental Sciences, University of Michigan, Ann Arbor, Michigan 48109, USA
[3]Department of Earth Sciences, University La Sapienza, Piazzale Aldo Moro, Rome 00185, Italy

ABSTRACT

The strength, shape, and ultimately seismic behavior of many thin-skinned fold and thrust belts, including marine accretionary wedges, are strongly controlled by large-scale faults that develop from weak, clay-rich sedimentary horizons (décollements). The increase of temperature with depth along clay-rich faults promotes the so-called smectite-illite transition, which may influence the fault strength, fluid distribution, and possibly the onset of seismicity. Here we report on the frictional properties of intact fault rocks retrieved from two large décollements, which were exhumed from depths above and below the smectite-illite transition. We find that all tested rocks are characterized by very low friction (μ = 0.17–0.26), velocity-strengthening behavior, and low rates of frictional healing, suggesting long-term fault weakness. Combining our experimental results with the critical taper theory, we computed the effective friction, *F*, of megathrusts beneath several accretionary wedges around the world; the result was extremely low (0.03 < *F* < 0.14), and in agreement with other independent estimates. Our analysis indicates a long-term weakness that can explain the shape of several tectonic wedges worldwide without invoking diffuse near-lithostatic fluid overpressures.

INTRODUCTION

Thin-skinned fold and thrust belts are characterized by the imbrication of thrust sheets that form wedge-shaped bodies above a sole thrust (décollement), leaving the underlying crystalline basement relatively undeformed (e.g., Bally et al., 1966; Fig. 1A). These faults localize in weak sedimentary horizons, usually within clay-rich sediments or salt (e.g., Morley and Guerin, 1996). The knowledge of the structure and mechanical properties of décollements is critical to the assessment of the shape and the strength of mountain belts and major crustal faults (Dahlen, 1990) and to understanding the seismicity of convergent tectonic settings.

Clay transformation from smectite to illite and cementation have been invoked to promote fault strengthening and to explain the onset of seismicity along megathrusts (Byrne et al., 1988; Vroljic, 1990; Moore and Saffer, 2001). However, experimental work on the sliding stability of illite powders demonstrated that progressive illitization may not be responsible for the aseismic-seismic transition (Saffer and Marone, 2003).

The strength of plate-boundary faults beneath fold and thrust belts inferred from the critical taper model or other energy balance models (e.g., Suppe, 2007) is approximately one order of magnitude lower than estimates obtained in the laboratory, i.e., friction, μ = 0.6–0.85 (Byerlee, 1978). Splay thrusts and basal décollements localized along weak sedimentary horizons show low friction (e.g., Ikari and Saffer, 2011; Remitti et al., 2015); however, most experiments have been performed on gouges retrieved from boreholes that can access only the shallowest part of the accretionary wedges, and therefore cannot shed light on the frictional strength of the deeper portions of these structures.

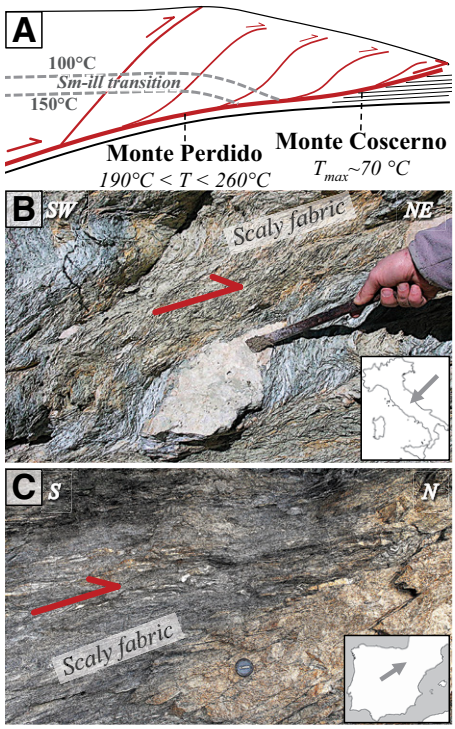

Figure 1. A: Schematic diagram of an accretionary wedge. Imbricated thrusts emanating from a sole décollement are localized in weak clay-rich lithologies (*T*—temperature). B: Detail of the block-in-matrix structure associated with the shallow Monte Coscerno thrust and the scaly fabric of the tectonic matrix. Inset shows location in Italy. C: Shear zone associated with the Monte Perdido thrust exhumed from depths below the smectite-illite (Sm-ill) transition. Note the resemblance of the two fault zones. Inset shows location in Spain (see the Data Repository [see footnote 1]). Lens cap is ~54 mm.

Here we show the results of friction experiments carried out on intact fault rocks collected from two large clay-rich faults exhumed from depths above and, for the first time, below the smectite-illite transition (Fig. 1). Furthermore, we incorporated our experimental results in the framework of the critical taper theory (Dahlen, 1990), proposing that nearly lithostatic fluid pressure is not needed to explain the shape of several accretionary prisms worldwide.

FAULT ZONE STRUCTURE

Clay-rich faults and tectonic mélanges are the best candidates to represent ancient décollements exposed at Earth's surface (e.g., Kimura et al., 2012). These structures are zones of highly sheared sediments with block-in-matrix structure in which the clay-rich matrix undergoes pervasive deformation and develops a typical scaly fabric (Moore et al., 1986; Festa et al., 2010).

In this study, the Monte Coscerno thrust (MCT) in the northern Apennines of Italy is taken as the analogue of the shallow portion of a décollement (depth < 5 km, temperature, *T* < 100 °C estimated reconstructing the stratigraphy overlying the fault; Tesei et al., 2014). Along the MCT, marls and marly limestones are incorporated into the fault zone, forming thick (20–200 m) shear zones characterized by disruption of the bedding and tectonic mixing of the formations. In these zones, distributed deformation in foliated rocks occurs synchronously with anastomosing localization features, suggesting inherent weakness of the shear zones (see details in the GSA Data Repository[1]). These rocks are characterized by pervasive S-CC' foliation, in which the shear surfaces are coated by smectite and envelop enclaves of poorly deformed marly protolith and boudinaged competent calcarenites (Fig. 1B).

In the Monte Perdido thrust (MPT), which crops out in the southern Pyrenees (Spain; Lacroix et al., 2011), a similar fault zone architecture develops from the tectonic disruption of

[1]GSA Data Repository item 2015309, details on location and structural characteristics of fault zones, mineralogical characterization of fault rocks, experimental details, and microstructures, is available online at www.geosociety.org/pubs/ft2015.htm, or on request from editing@geosociety.org or Documents Secretary, GSA, P.O. Box 9140, Boulder, CO 80301, USA.

clay-rich turbidites, in which S-CC' tectonites constitute the flowing matrix of relatively more competent sandstone boudins and shear veins (Fig. 1C). The clay mineralogy along the shear surfaces is represented by illite and syntectonic chlorite that precipitated at T ~240 °C and depth > 5 km (from compositional thermometry; Lacroix et al., 2011); therefore, the MPT can represent a décollement exhumed from below the smectite-illite transition.

In both cases, clays outlining the scaly fabric occur along smooth and continuous seams that are mostly decorated by slickenlines and slickenfibers, evidencing frictional sliding along the foliation. In addition, the presence of veins and newly formed minerals indicates multiple cycles of fluid pressure fluctuations and cementation along the studied fault zones.

EXPERIMENTAL RESULTS

We performed 13 friction experiments on rectangular wafers of intact fault rocks from the MCT and MPT (26 samples, 50 × 50 mm, ~12 mm thick), reshearing the natural scaly fabric (e.g., Collettini et al., 2009). MCT fault rocks contain ~35% smectite, whereas in MPT chlorite and illite form ~50% of the rock volume (for details, see the Data Repository). We also performed nine experiments on powders (8 mm thick) derived from the same samples to show the difference in friction induced by the disruption of the natural fabric. Experiments were performed in a biaxial apparatus (Collettini et al., 2014) in a double-direct shear configuration (Fig. 2A, inset), in which two samples are simultaneously sheared. Each test was carried out at a shearing velocity of 10 µm/s at normal stresses from 6 to 100 MPa. We also conducted velocity stepping and slide-hold-slide sequences to study the frictional response to fault acceleration and frictional healing after simulated interseismic periods. Experiments were performed under water submersion (complete saturation) and room-temperature conditions (for further details, see the Data Repository). We measured the shear stress (τ) during steady-state sliding of the rocks, which varies linearly with the applied normal stress (σ_n), consistently with a Coulomb-type brittle failure envelope (Fig. 2A):

$$\tau = \mu\sigma_n + C, \quad (1)$$

where C is the cohesion of the rocks, and was negligible.

All wafers are frictionally weaker than typical crustal fault rocks, i.e., $\mu << 0.6$ (Byerlee, 1978), and the average friction of illite-chlorite–rich wafers ($\mu = 0.17$) is even lower than the friction of smectite-rich wafers ($\mu = 0.26$). Even though fault rock wafers show abundant veining due to syntectonic precipitation of strong mineral phases such as calcite (e.g., Figs. 2D and 2E), their friction is lower than powdered standards or illite-rich sediments (Morrow et al., 1992; Saffer et al., 2012).

Microstructural studies of preexperimental and postexperimental faults (Figs. 2D and 2E; see the Data Repository) document that the sliding was accommodated along the interconnected phyllosilicate horizons with limited deformation of the intervening material, resulting in a significant frictional weakness (e.g., Holdsworth, 2004). The MPT illite-chlorite–rich rocks (Fig. 2D) are more clay rich and exhibit a more pervasive foliation with respect to the MCT rocks (Fig. 2E), resulting in lower friction. Low friction, maintained in the presence of fault-parallel veins, indicates that in thick phyllosilicate-rich fault zones the volumetric increase of strong minerals (calcite and quartz) or cementation processes might not be an efficient mechanism for fault strengthening. Our data suggest that the smectite-illite transition and cementation processes are not responsible for a possible increase in fault strength with depth, but the sample strength is mostly ruled by the intensity and connectivity of the foliation.

In addition, both MCT and MPT rocks display a velocity-strengthening friction during velocity stepping tests with (a-b) values ranging from 0.003 to 0.011 and constant b values close to zero (Fig. 2B). Such (a-b) values are substantially insensible to difference in normal stress or phyllosilicate mineralogy and suggest unfavorable conditions for earthquake nucleation during the shearing of clay-rich matrixes of décollements. Furthermore, these rocks lack frictional healing, i.e., peak frictional strength

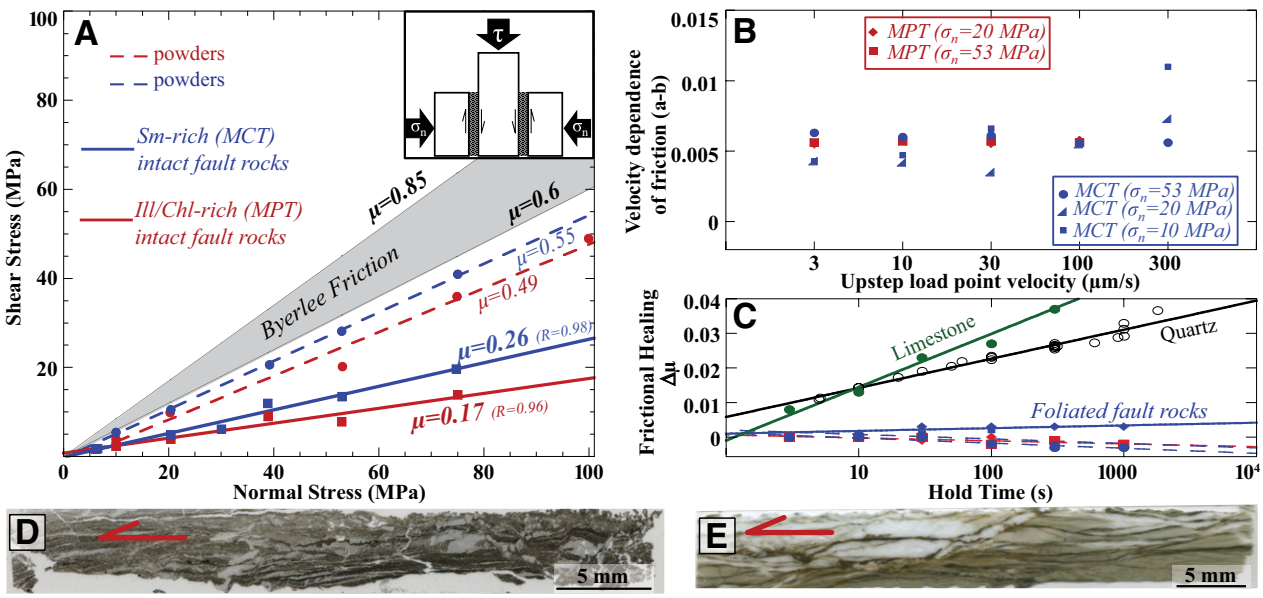

Figure 2. A: Steady-state shear stress (τ) versus normal stress (σ_n) for smectite-rich (Sm) and illite-chlorite–rich (Ill/Chl) fault rocks. Foliated fault rocks from the Monte Coscerno thrust (MCT; northern Apennines, Italy) display average friction μ = 0.26, whereas Monte Perdido thrust (MPT; southern Pyrenees, Spain) rocks show μ = 0.17. Friction of powders of the same fault rocks and Byerlee friction are shown for comparison. Inset: Double direct shear configuration. B: Velocity dependence of friction of foliated rocks under different applied normal stresses. C: Frictional healing of décollement fault rocks compared to quartz (Marone, 1998) and calcite (Tesei et al., 2014) powders. D: Postexperimental microstructure of MPT samples. The survival of intact sigmoidal lithons and syntectonic veins indicates that shear is accommodated along the S-CC' fabric (see text). E: Postexperimental microstructure of MCT samples.

upon reshearing after experimental periods of no slip (Fig. 2C).

All the above properties of intact foliated rocks across the smectite-illite transition depict a fault material characterized by inherently stable friction, with limited effects of cementation, low frictional healing, and thus long-term weakness. As a consequence, other processes have to be invoked to explain the onset of seismicity observed at the depth of the smectite-illite transition. For example, the disruption of the foliation and gouge production caused by prolonged shear and extensive veining, or the presence of lithological heterogeneities, might cause an increase in the ratio of competent versus incompetent materials in the fault zone and an increase in rock friction (e.g., from wafers to powders friction; Fig. 2A). These processes might result in higher strain rates in the weak matrix (Fagereng and Sibson, 2010) and/or brittle localization in strong materials characterized by velocity-weakening behavior (e.g., Blanpied et al., 1998), promoting earthquake nucleation.

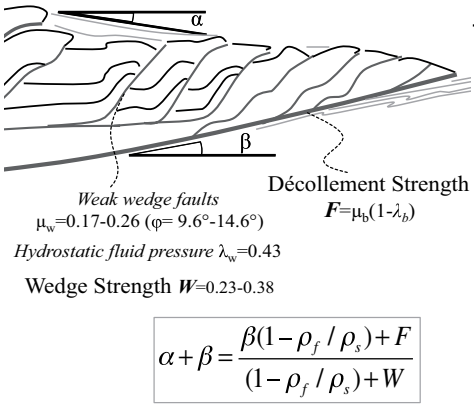

Wedge	α	β	F (W=0.23)	F (W=0.38)	λ_b (μ_b=0.17-0.26)
Barbados	3°	2°	0.05	0.06	0.7<λ_b<0.8
Cascadia	1.1°	2.8°	0.03	0.04	λ_b~0.8
Hikurangi (South)	1°	3°	0.03	0.04	λ_b~0.8
Makran	2°	2.5°	0.04	0.05	λ_b~0.8
Nankai (East)	1.5°	2.6°	0.03	0.04	λ_b~0.8
Sumatra (South)	2°	3°	0.04	0.05	0.7<λ_b<0.8
Taiwan	2°	2.7°	0.04	0.05	0.7<λ_b<0.8
Aleutians	3.4°	3.9°	0.06	0.08	0.6<λ_b<0.7
Low tapers			***0.03<F<0.06***		$\lambda_b \leq 0.8$
Chile (South)	5°	6°	0.09	0.12	0.4<λ_b<0.6
Costa Rica	3.5°	6°	0.07	0.10	0.5<λ_b<0.6
Java	3.1°	6°	0.07	0.09	0.5<λ_b≤0.6
Kurile (South)	1.3°	9.7°	0.06	0.09	λ_b~0.6
Kermadek	3.7°	6.8°	0.08	0.11	0.5<λ_b<0.6
Hikurangi (North)	3.5°	7.5°	0.08	0.11	0.5<λ_b<0.6
Nankai (West)	5°	3°	0.08	0.10	0.5<λ_b<0.6
Peru	6.5°	4°	0.11	0.14	0.3<λ_b<0.5
Moderate tapers			***0.06<F<0.14***		λ_b<0.6

Figure 3. Left: Critical taper parameters (after Suppe, 2007); rock friction from Figure 2A and hydrostatic fluid pressure have been assumed to compute wedge strength *W*. Right: décollement strength (*F*) and basal fluid pressure ratio λ_b of several accretionary wedges worldwide calculated with Equation 2 using our friction data and wedge average slope, α, and décollement dip, β, angles (for references on the wedge geometry, see the Data Repository [see footnote 1]).

FRICTIONAL STRENGTH VERSUS CRITICAL TAPER MECHANICS

The experimental data can be incorporated into the framework of the critical taper theory (Davis et al., 1983; Dahlen, 1990) to constrain the strength of thin-skinned fold and thrust belts and their décollements from the wedge geometry. The assumption of the theory is that the taper angle of an accretionary wedge is the result of the long-term mechanical equilibrium between internal deformation of the wedge, which is everywhere on the verge of failure, and the sliding along the weak basal décollement. Following Dahlen (1990) and Suppe (2007), the critical taper of a cohesionless wedge can be expressed as:

$$\alpha+\beta=\left[\beta\left(1-\rho_f/\rho_s\right)+F\right]/\left[\left(1-\rho_f/\rho_s\right)+W\right], \quad (2)$$

where α is the slope of the top of the wedge, β is the dip of the décollement (Fig. 3), and ρ_f/ρ_s is the ratio between density of the fluid overlying the wedge (water or air) and the mean wedge rock density. *F* and *W* are the décollement and wedge strength terms, respectively, where $F = \mu_b(1 - \lambda_b)$ is the décollement effective friction, and $W = 2(1 - \lambda_w)(\sin\varphi/1 - \sin\varphi)$ is the normalized differential stress at failure; φ is the internal friction angle of the wedge material, and $\tan\varphi = \mu_w(1 - \lambda_w)$, where μ_w is the friction coefficient of the wedge rocks. λ_w and λ_b are the depth-normalized fluid pressures in the wedge and décollement, respectively.

From Equation 2, given the average α and β angles, the set of all possible *F* and *W* strengths are along a single line with slope (α + β); to constrain *F*, *W* has to be determined, and vice versa (e.g., Suppe, 2007). Commonly, *F* and *W* have been calculated by assuming the fluid pressure λ_w or λ_b from well data or seismological inversions, and using standard values of rock friction, $\mu \approx 0.6–1$ (e.g., Davis et al., 1983).

In the following we estimate via Equation 2 the décollement strength *F* and fluid pressure ratio λ_b in several wedges throughout the world by using rock friction values (determined in the previous section; Figs. 2 and 3).

To compute the buoyancy terms in Equation 2, we adopted an average sediment density, ρ_s = 2300 kg/m^3, and fluid density, ρ_w = 1000 kg/m^3 (water), whereas α and β are average values reported in the literature for several accretionary wedges having décollements likely hosted in clay-rich sediments (for references, see the Data Repository). To constrain *W*, we propose that the internal deformation of wedges is not homogeneous, but mostly dominated by sliding along mature faults that are significantly weaker than the bulk wedge material. Such long-lived structures develop scaly fabrics similar to those of the MCT and MPT faults, as documented by scientific drillings (e.g., Moore et al., 1986) and exhumed analogues (e.g., Festa et al., 2010). In addition, friction experiments performed on unlithified fault materials from shallow levels of accretionary wedges show low friction, $\mu \leq 0.3$ (Ikari and Saffer, 2011). Assuming weak wedge faults with friction constrained by our lab experiments, i.e., $\mu = 0.17–0.26$, the corresponding wedge internal friction angles are $\varphi = 9.6°–14.6°$, that result in $W = 0.23–0.38$ for simple hydrostatic fluid pressure in the wedge ($\lambda_w = 0.43$). Under these assumptions, we compute the décollement strength *F* of all wedges in the range $0.03 < F < 0.14$ (Fig. 3). All these décollements are extremely weak, but nonetheless are widely consistent with estimations of plate boundary fault strengths independently derived from stress orientations (e.g., Mount and Suppe, 1987), force balancing (e.g., Wang and He, 1999; Lamb, 2006), heat flow modeling (Gao and Wang, 2014), and analysis of wedge tapers (Suppe, 2007).

The *F* values highlight two groups of wedges: one with $0.06 < F < 0.14$ that includes moderately tapered wedges with $\alpha + \beta \geq 8°$ (see Fig. 3), and one with $0.03 < F < 0.06$ corresponding to low-tapered wedges with $\alpha + \beta \leq 7°$ (Fig. 3). If we assume that the friction of décollement rocks is also similar to the one we measured in laboratory experiments, $\mu_b = 0.17–0.26$, we compute a décollement fluid pressure ratio $\lambda_b < 0.6$ for moderately tapered wedges and $\lambda_b \leq 0.8$ for low-tapered wedges (Fig. 3).

Our analysis shows that widespread nearly lithostatic fluid pressure is not needed to explain the shape of several active prisms worldwide as long as low friction of foliated fault rocks is taken into account both in the basal décollement and in the wedge. Significant fluid overpressure is required only within the décollement of low tapered wedges with values not exceeding $\lambda_b \sim 0.8$.

In many previous applications of the critical taper theory, friction has been assumed equal in both wedge and décollement ($\mu_w = \mu_b$), within the experimental range of 0.6–1 (e.g., Davis et al., 1983; Suppe, 2007) or slightly reduced in the décollement, such as $\mu_b < \mu$ (e.g., Fagereng, 2011). Under these assumptions of high friction in the wedge and in the décollement, the critical taper theory predicts that large overpressures are required to model the shape of many accretionary wedges, i.e., λ_w and λ_b in excess of 0.7, and in some cases $\lambda > 0.9$ near the lithostatic limit (e.g., Davis et al., 1983). Such high overpressures are usually explained by disequilibrium compaction of sediments, during which pore fluids are trapped in low-permeability rocks that undergo rapid increase of overburden and tectonic load (Tobin and Saffer, 2009).

However, in pervasively deforming regions like fold and thrust belts, it is likely that high fluid

overpressure might be relaxed by faulting over long geological times (Townend and Zoback, 2000). Therefore, it is reasonable to consider the wedges close to hydrostatic conditions in the long term, whereas continuous décollements may act as physical barriers to fluid migration, maintaining a pressure discontinuity ($\lambda_b > \lambda_w$).

In some well-studied convergent settings, such as the Nankai prism and the Taiwan orogen, fluid overpressures have been constrained by inversion of seismological data (Tobin and Saffer, 2009) and by extrapolation of well fluid pressures, assuming disequilibrium compaction (Yue and Suppe, 2014). Note that these estimations suggest fluid overpressure in the range of 75%–80% of the lithostatic load at the level of the main tectonic décollements, in good agreement with our estimations of $0.7 < \lambda_b \leq 0.8$.

We also note that the critical taper theory models the long-term deformation, thus averaging short-term deformations like earthquakes. Very low *F* values might be due to earthquake dynamic weakening (Rice 2006) rather than long-lived high fluid pressures (Wang and Hu, 2006).

In conclusion, the frictional properties of clay-rich faults, commonly occurring in thin-skinned fold and thrust belts, are likely to be scarcely affected by mineralogical transformations of clays and cementation with increasing depth. Conversely, their weakness helps to explain the shape and strength of several tectonic wedges worldwide without invoking long-term and diffuse near-lithostatic fluid overpressures.

ACKNOWLEDGMENTS

This research was carried out within the European Research Council research starting grant 259256 (GLASS project). We thank Matt Ikari and two anonymous reviewers for very constructive reviews.

REFERENCES CITED

Bally, A.W., Gordy, P.L., and Stewart, G.A., 1966, Structure, seismic data and orogenic evolution of southern Canadian Rocky Mountains: Bulletin of Canadian Petroleum Geology, v. 14, p. 337–381.

Blanpied, M.L., Marone, C., Lockner, D.A., Byerlee, J.D., and King, D.P., 1998, Quantitative measure of variation in fault rheology due to fluid-rock interactions: Journal of Geophysical Research, v. 103, no. B5, p. 9691–9712, doi:10.1029/98JB00162.

Byerlee, J., 1978, Friction of rocks: Pure and Applied Geophysics, v. 116, p. 615–626, doi:10.1007/BF00876528.

Byrne, D.E., Davis, D.M., and Sykes, L.R., 1988, Loci and maximum size of thrust earthquakes and mechanics of the shallow region of subduction zones: Tectonics, v. 7, p. 833–857, doi:10.1029/TC007i004p00833.

Collettini, C., Niemeijer, A., Viti, C., and Marone, C., 2009, Fault zone fabric and fault weakness: Nature, v. 462, p. 907–910, doi:10.1038/nature08585.

Collettini, C., Di Stefano, G., Carpenter, B., Scarlato, P., Tesei, T., Mollo, S., Trippetta, F., Marone, C., Romeo, G., and Chiaraluce, L., 2014, A novel and versatile apparatus for brittle rock deformation: International Journal of Rock Mechanics and Mining Sciences, v. 66, p. 114–123, doi:10.1016/j.ijrmms.2013.12.005.

Dahlen, F.A., 1990, Critical taper model of fold-and-thrust belts and accretionary wedges: Annual Review of Earth and Planetary Sciences, v. 18, p. 55–99, doi:10.1146/annurev.ea.18.050190.000415.

Davis, D., Suppe, J., and Dahlen, F.A., 1983, Mechanics of fold-and-thrust belts and accretionary wedges: Journal of Geophysical Research, v. 88, no. B2, p. 1153–1172, doi:10.1029/JB088iB02p01153.

Fagereng, A., 2011, Wedge geometry, mechanical strength, and interseismic coupling of the Hikurangi subduction thrust, New Zealand: Tectonophysics, v. 507, p. 26–30, doi:10.1016/j.tecto.2011.05.004.

Fagereng, A., and Sibson, R.H., 2010, Mélange rheology and seismic style: Geology, v. 38, p. 751–754, doi:10.1130/G30868.1.

Festa, A., Pini, G.A., Dilek, Y., and Codegone, G., 2010, Mélanges and mélange-forming processes: A historical overview and new concepts: International Geology Review, v. 52, p. 1040–1105, doi:10.1080/00206810903557704.

Gao, X., and Wang, K., 2014, Strength of stick-slip and creeping subduction megathrusts from heat flow observations: Science, v. 345, p. 1038–1041, doi:10.1126/science.1255487.

Holdsworth, R.E., 2004, Weak faults—Rotten cores: Science, v. 303, p. 181–182, doi:10.1126/science.1092491.

Ikari, M.J., Saffer, D.M., 2011, Comparison of frictional strength and velocity dependence between fault zones in the Nankai accretionary complex: Geochemistry, Geophysics, Geosystems, v. 12, Q0AD11, doi:10.1029/2010GC003442.

Kimura, G., Yamaguchi, A., Hojo, M., Kitamura, Y., Kameda, J., Ujiie, K., Hamada, Y., Hamahashi, M., and Hina, H., 2012, Tectonic mélange as fault rock of subduction plate boundary: Tectonophysics, v. 568–569, p. 25–38, doi:10.1016/j.tecto.2011.08.025.

Lacroix, B., Buatier, M., Labaume, P., Travé, A., Dubois, M., Charpentier, D., Ventalon, S., and Convert-Gaubier, D., 2011, Microtectonic and geochemical characterization of thrusting in a foreland basin: Example of the South Pyrenean orogenic wedge (Spain): Journal of Structural Geology, v. 33, p. 1359–1377, doi:10.1016/j.jsg.2011.06.006.

Lamb, S., 2006, Shear stresses on megathrusts: Implications for mountain building behind subduction zones: Journal of Geophysical Research, v. 111, B07401, doi:10.1029/2005JB003916.

Marone, C., 1998, Laboratory-derived friction laws and their application to seismic faulting: Annual Review of Earth and Planetary Sciences, v. 26, p. 643–696, doi:10.1146/annurev.earth.26.1.643.

Moore, J.C., and Saffer, D.M., 2001, Updip limit of the seismogenic zone beneath the accretionary prism of southwest Japan: An effect of diagenetic to low-grade metamorphic processes and increasing effective stress: Geology, v. 29, p. 183–186, doi:10.1130/0091-7613(2001)029<0183:ULOTSZ>2.0.CO;2.

Moore, J.C., Roeske, S., Cowan, D.S., Lundberg, N., Gonzales, E., Schoonmaker, J., and Lucas, S.E., 1986, Scaly fabrics from Deep Sea Drilling Project cores from forearcs, *in* Moore, J.C., ed., Structural fabrics in Deep Sea Drilling Project cores from forearcs: Geological Society of America Memoir 166, p. 55–74, doi:10.1130/MEM166-p55.

Morley, C.K., and Guerin, G., 1996, Comparison of gravity-driven deformation styles and behavior associated with mobile shales and salt: Tectonics, v. 15, p. 1154–1170, doi:10.1029/96TC01416.

Morrow, C., Radney, B., and Byerlee, J., 1992, Frictional strength and the effective pressure law of montmorillonite and illite clays, *in* Evans, B., and Wong, T.-F., eds., Fault mechanics and transport properties of rocks: International Geophysics, v. 51, p. 69–88, doi:10.1016/S0074-6142(08)62815-6.

Mount, V.S., and Suppe, J., 1987, State of stress near the San Andreas fault: Implications for wrench tectonics: Geology, v. 15, p. 1143–1146, doi:10.1130/0091-7613(1987)15<1143:SOSNTS>2.0.CO;2.

Remitti, F., Smith, S.A.F., Mittempergher, S., Gualtieri, A.F., and Di Toro, G., 2015, Frictional properties of fault zone gouges from the J-FAST drilling project (M_w 9.0 2011 Tohoku-Oki earthquake): Geophysical Research Letters, v. 42, p. 2691–2699, doi:10.1002/2015GL063507.

Rice, J.R., 2006, Heating and weakening of faults during earthquake slip: Journal of Geophysical Research, v. 111, B05311, doi:10.1029/2005JB004006.

Saffer, D.M., and Marone, C., 2003, Comparison of smectite- and illite-rick gouge frictional properties: Application to the updip limit of the seismogenic zone along subduction megathrusts: Earth and Planetary Science Letters, v. 215, p. 219–235, doi:10.1016/S0012-821X(03)00424-2.

Saffer, D.M., Lockner, D.A., and McKiernan, A., 2012, Effects of smectite to illite transformation on the frictional strength and sliding stability of intact marine mudstones: Geophysical Research Letters, v. 39, L11304, doi:10.1029/2012GL051761.

Suppe, J., 2007, Absolute fault and crustal strength from wedge tapers: Geology, v. 35, p. 1127–1130, doi:10.1130/G24053A.1.

Tesei, T., Collettini, C., Barchi, M.R., Carpenter, B.M., and Di Stefano, G., 2014, Heterogeneous strength and fault zone complexity of carbonate-bearing thrusts with possible implications for seismicity: Earth and Planetary Science Letters, v. 408, p. 307–318, doi:10.1016/j.epsl.2014.10.021.

Tobin, H.J., and Saffer, D.M., 2009, Elevated fluid pressure and extreme mechanical weakness of a plate boundary thrust, Nankai Trough subduction zone: Geology, v. 37, p. 679–682, doi:10.1130/G25752A.1.

Townend, J., and Zoback, M.D., 2000, How faulting keeps the crust strong: Geology, v. 28, p. 399–402, doi:10.1130/0091-7613(2000)28<399:HFKTCS>2.0.CO;2.

Vroljic, P., 1990, On the mechanical role of smectite in subduction zones: Geology, v. 18, p. 703–707, doi:10.1130/0091-7613(1990)018<0703:OTMROS>2.3.CO;2.

Wang, K., and He, J., 1999, Mechanics of low-stress forearcs: Nankai and Cascadia: Journal of Geophysical Research, v. 104, no. B7, p. 15,191–15,205, doi:10.1029/1999JB900103.

Wang, K., and Hu, Y., 2006, Accretionary prisms in subduction earthquake cycles: The theory of dynamic Coulomb wedge: Journal of Geophysical Research, v. 111, B06410, doi:10.1029/2005JB004094.

Yue, L.-F., and Suppe, J., 2014, Regional pore-fluid pressure in the active western Taiwan thrust belt: A test of the classic Hubbert-Rubey fault-weakening hypothesis: Journal of Structural Geology, v. 69, p. 493–518, doi:10.1016/j.jsg.2014.08.002.

Manuscript received 17 May 2015
Revised manuscript received 11 August 2015
Manuscript accepted 13 August 2015

Printed in USA